ACS APPLIED MATERIALS & INTERFACES

Research Article

www.acsami.org

Efficient Catalytic Reduction of Hexavalent Chromium Using Palladium Nanoparticle-Immobilized Electrospun Polymer Nanofibers

Yunpeng Huang,[†,‡] Hui Ma,[‡] Shige Wang,[§] Mingwu Shen,*[,‡] Rui Guo,[‡] Xueyan Cao,[‡] Meifang Zhu,[†] and Xiangyang Shi*[,†,‡,⊥]

[†]State Key Laboratory for Modification of Chemical Fibers and Polymer Materials, [‡]College of Chemistry, Chemical Engineering and Biotechnology, and [§]College of Materials Science and Engineering, Donghua University, Shanghai 201620, People's Republic of China

[⊥]CQM-Centro de Química da Madeira, Universidade da Madeira, Campus da Penteada, 9000-390 Funchal, Portugal

Supporting Information

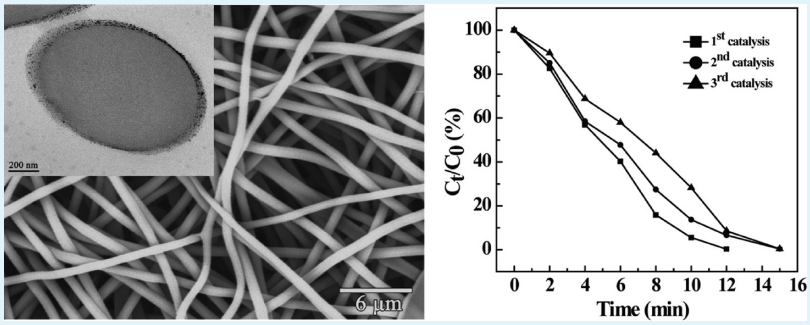

ABSTRACT: We report a facile and economic approach to fabricating catalytic active palladium (Pd) nanoparticle (NP)-immobilized electrospun polyethyleneimine (PEI)/polyvinyl alcohol (PVA) nanofibers for catalytic reduction of hexavalent chromium (Cr(VI)) to trivalent chromium (Cr(III)). In this study, PEI/PVA nanofibrous mats were first electrospun from homogeneous mixture solution of PEI and PVA, followed by cross-linking with glutaraldehyde vapor to render the fibers with good water stability. The nanofibrous mats were then alternatively soaked in potassium tetrachloropallidate (K_2PdCl_4) and sodium borohydride solution, and the $PdCl_4^{2-}$ anions complexed with the free amine groups of PEI were able to be reduced to form zero-valent Pd NPs. The formed Pd NP-containing PEI/PVA nanofibers were characterized by different techniques. We show that the immobilization of Pd NPs does not significantly change the morphology of the PEI/PVA nanofibers; instead the mechanical durability of the fibers is significantly improved. The formed Pd NPs with a mean diameter of 2.6 nm are quite uniformly distributed within the fibers with a small portion of particles having a denser distribution at the outer surface of the fibers. The catalytic activity and reusability of the fabricated Pd NP-containing fibrous mats were evaluated by transformation of Cr(VI) to Cr(III) in aqueous solution in the presence of a reducing agent. Our results reveal that the Pd NP-containing nanofibrous mats display an excellent catalytic activity and reusability for the reduction of Cr(VI) to Cr(III). The facile approach to fabricating metal NP-immobilized polymer nanofibers with a high surface area to volume ratio, enhanced mechanical durability, and uniform NP distribution may be extended to prepare different NP-immobilized fibrous systems for various applications in catalysis, sensing, environmental sciences, and biomedicine.

KEYWORDS: *electrospun PEI/PVA nanofibers, palladium nanoparticles, hexavalent chromium reduction, environmental remediation, reusable catalyst*

INTRODUCTION

Hexavalent chromium (Cr(VI)) compounds have been considered to be one of the most common pollutants and have been proven to have acute toxicity and mutagenicity and carcinogenicity as well.[1,2] In contrast, trivalent chromium (Cr(III)) is less toxic and less mobile in nature, and trace amounts of Cr(III) have been considered to be an essential nutrient required for sugar and lipid metabolism for human and animal. Therefore, for environmental cleanup of the abandoned Cr(VI) production sites to mitigate hazardous impact on health, it is essential to develop different technologies to transform Cr(VI) to Cr(III).

Recently, some practical and economic techniques have been developed to reduce Cr(VI) to Cr(III).[3−5] For instance,

Received: March 7, 2012
Accepted: May 16, 2012
Published: May 16, 2012

Daneshvar et al.[6] used soya cake as the reductant and observed a high efficiency in reduction of Cr(VI) to Cr (III). Puzon et al.[7] investigated the reduction of Cr(VI) using a bacterial enzyme system and a reductant NADH, and the cellular organic metabolites were able to convert Cr(VI) to both soluble and insoluble organo-Cr(III) end-products. Beyond the biological approaches, noble metal nanoparticles (NPs) have received much attention to be used as environmental catalysts.[8−11] In a recent study, Sadik and coworkers[12] used colloidal Pd NPs as a catalyst and formic acid as a reducing agent to achieve an efficient reduction of Cr(VI) to Cr(III). To make the Pd NPs as reusable catalysts for Cr(VI) reduction, Dandapat et al.[13] used relatively thick Pd NP-incorporated mesoporous γ-Al_2O_3 films as a catalyst to transform Cr(VI) to Cr(III) in the presence of formic acid. These studies clearly suggest that Pd NPs could be used as an efficient catalyst for environmental remediation of Cr(VI). More importantly, due to the rarity of metal Pd and the further possible environmental contamination risk of colloidal Pd NPs in aqueous media or soil, the separation and reuse of the costly Pd NPs are crucial. Therefore, development of various supporting materials that are able to efficiently immobilize Pd NPs and retain their catalytic activity is necessary for practical environmental remediation applications.

Electrospinning has been considered as one of the powerful methods to generate polymer fibers with the diameter ranging from tens of nanometers to several micrometers.[14,15] Through this facile and low-cost strategy, various polymeric nanofibers and nanostructured materials with a high aspect ratio and a specific surface area[16−18] have been fabricated for various applications including but not limited to solar cells,[19] filtration,[20] environmental remediation,[18,21−23] protective clothing,[24] biosensors,[25] and tissue engineering scaffolds.[26−31] Recent studies in our laboratory have shown that electrospun polyacrylic acid (PAA)/polyvinyl alcohol (PVA) nanofibers can be used as a promising nanoreactor to immobilize zero-valent iron NPs for environmental remediation applications with high activity and reusability.[32−34] In our another work, we have shown that electrospun polyethyleneimine (PEI)/PVA nanofibers can be used as a nanoreactor for in situ formation of gold NPs (AuNPs).[9] The formed AuNP-immobilized polymer nanofibers have been demonstrated to be a highly active and reusable catalyst in the transformation of 4-nitrophenol to 4-aminophenol in the presence of sodium borohydride ($NaBH_4$). These successes in the immobilization of metal Fe or Au within electrospun polymer nanofibers lead us to develop a facile approach to immobilizing Pd NPs within the polymer nanofibers for catalytic transformation of Cr(VI) to Cr(III).

In this present study, uniform electrospun PEI/PVA nanofibers were first cross-linked via glutaraldehyde (GA) vapor treatment to gain good water stability. The water-stable electrospun PEI/PVA nanofibers were then exposed to a potassium tetrachloropallidate (K_2PdCl_4) water solution to complex the $PdCl_4^{2-}$ anions with the free PEI amine groups of the PEI/PVA nanofibers. Following a $NaBH_4$ reduction reaction, Pd NPs were formed and immobilized within the nanofibers (Figure 1). The morphology and composition of the formed Pd NP-containing nanofibers were characterized using scanning electron microscopy (SEM), transmission electron microscopy (TEM), energy dispersive spectroscopy (EDS), Fourier transform infrared (FTIR) spectroscopy, and thermal gravimetric analysis (TGA). The catalytic activity of the Pd NP-immobilized PEI/PVA nanofibrous mat was investigated by

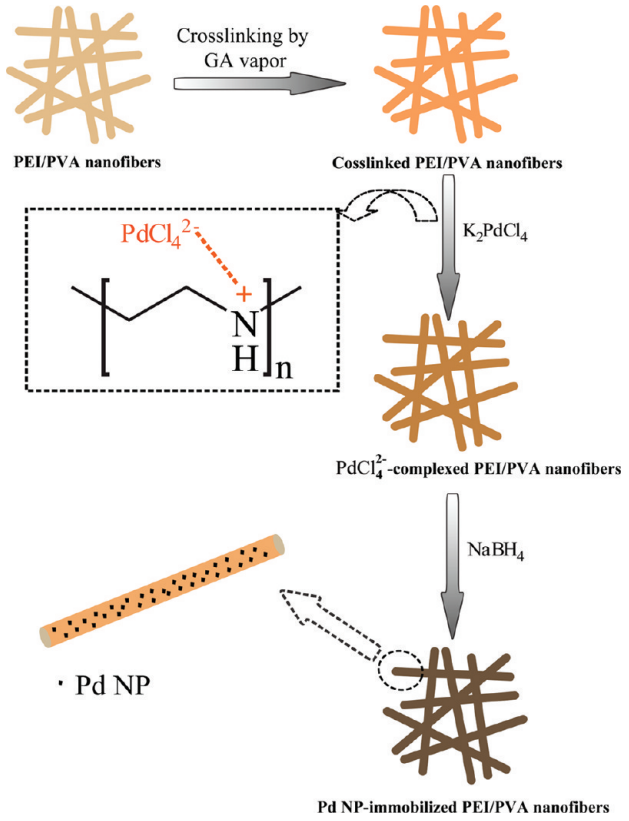

Figure 1. Schematic illustration of the immobilization of Pd NPs within the electrospun PEI/PVA nanofibers.

reducing Cr(VI) to Cr(III) in the presence of formic acid. The reusability of these Pd NP-containing nanofibrous mats was also evaluated. To the best of our knowledge, this is the first report related to the fabrication of Pd NP-immobilized electrospun polymer nanofibrous mats for catalytic transformation of Cr(VI) to Cr(III).

EXPERIMENTAL SECTION

Materials. PEI (branched, M_w = 750 000, 50% in water) was purchased from Sigma-Aldrich. PVA (88% hydrolyzed, M_w = 88 000) and $NaBH_4$ were obtained from J&K chemical. K_2PdCl_4 was acquired from Alfa Aesar. Other chemicals including GA (25%), potassium dichromate ($K_2Cr_2O_7$), and formic acid were purchased from Sinopharm Chemical Reagent Co., Ltd. (China). All chemicals were used as received. Water used in all experiments was purified using a Milli-Q Plus 185 water purification system (Millipore, Bedford, MA) with resistivity higher than 18 MΩ cm.

Preparation of PEI/PVA Nanofibrous Mats. The electrospun PEI/PVA nanofibers were prepared according to the protocol reported in our previous study[9] but with a commercial electrospinning equipment (1006 Electrospinning equipment, Beijing Kang Sente Technology Co., Ltd., Beijing, China). Briefly, PEI (50 wt %) and PVA (12 wt %) solutions were mixed together under magnetic stirring overnight with a PEI/PVA mass ratio of 1:3 to achieve a homogeneous solution. The freshly prepared polymer solution was pumped into a syringe with a needle having an inner diameter of 0.8 mm. The flow rate was controlled by a syringe pump at 0.3 mL/h. The high voltage power supplier was connected to the needle by a high-voltage insulating wire with two clamps at the end. An aluminum (Al) board covered with Al foil positioned vertically was used as the collector and was connected to the ground. The distance between the needle tip and the collector was set at 25 cm and the operating voltage was set at 18.6 kV. The formed nanofibrous mats were vacuum dried for 24 h before further treatment.

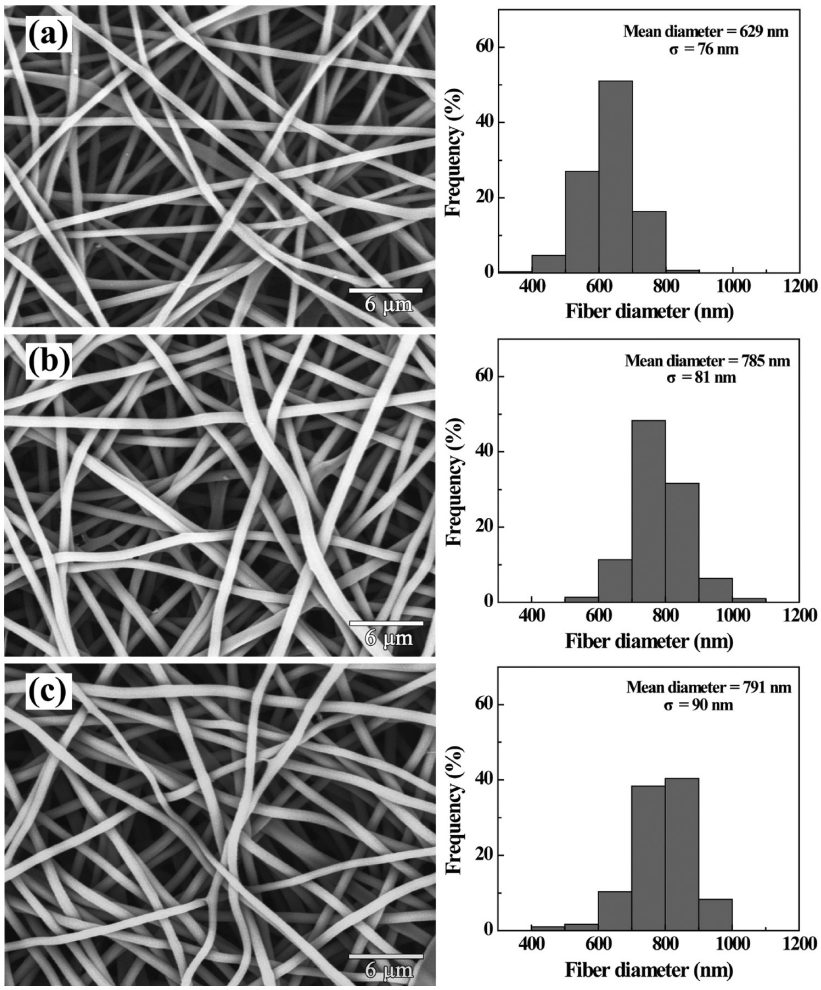

Figure 2. SEM images and diameter distribution histograms of (a) the non-cross-linked PEI/PVA nanofibers, (b) the cross-linked PEI/PVA nanofibers, and (c) the Pd NP-containing PEI/PVA nanofibers.

The freshly prepared PEI/PVA nanofibers were then cross-linked by GA vapor to render the fibers with water stability.[35] In brief, a Petri dish containing GA solution (20 mL, 25% in aqueous solution) was first placed at the bottom of a vacuum desiccator, then the electrospun PEI/PVA nanofibrous mats on Al foil were put onto the ceramic plate inside the desiccator, followed by application of vacuum for 24 h. The mats on Al foil were then withdrawn and immersed into water for several minutes to make them detached from the Al foil. The freestanding nanofibrous mats were then washed with water 3 times to remove excess GA. Then the fibrous mats were dried under vacuum and stored in a desiccator before use.

Immobilization of Pd NPs within PEI/PVA Nanofibrous Mats. The process to immobilize Pd NPs within the cross-linked PEI/PVA nanofibers is schematically shown in Figure 1. Briefly, a piece of cross-linked water-stable PEI/PVA nanofibrous mat (8×8 cm^2, 130 mg) was immersed into a K_2PdCl_4 aqueous solution (4 mM, 40 mL) for 1 h to allow $PdCl_4^{-2}$ ions to be complexed with the available PEI amine groups through ionic exchange, followed by rinsing with water for 3 times to remove excess $PdCl_4^{2-}$ ions. Then $NaBH_4$ solution (20 mM, 40 mL) was dropwise (2 drops/3 s) added onto the nanofibrous mat to reduce $PdCl_4^{2-}$ ions until there was no hydrogen gas to release. The formed Pd NP-containing nanofibrous mats were rinsed 3 times with water, followed by vacuum drying at room temperature for 24 h. Finally, the nanofibrous mats were stored in a desiccator before use.

Characterization Techniques. The morphology of the electrospun PEI/PVA nanofibrous mats before and after Pd NP immobilization was observed using SEM (JSM-5600LV, JEOL Ltd., Japan) with an operating voltage of 15 kV. Prior to SEM measurements, samples were sputter-coated with 10 nm thick carbon films. The elemental composition of the samples was analyzed by EDS (IE300X, Oxford, U.K.) attached to the SEM. To observe the size distribution of Pd NPs in the nanofibers, the Pd NP-containing polymer nanofibrous mats were embedded in epoxy resin and were cut into ultrathin sections with ultramicrotome equipped with a diamond knife. The cross-sectional image of the fibers containing Pd NPs was imaged using TEM (JEM2100, JEOL Ltd., Japan) with an operating voltage of 200 kV. The diameters of nanofibers and particle sizes were measured using image analysis software ImageJ 1.40G (http://rsb.info.nih.gov/ij/download.html). At least 300 randomly selected nanofibers or Pd NPs in different SEM or TEM images were analyzed for each sample in order to acquire the diameter or size distribution histograms. TGA was carried out between 20 and 750 °C on a TG 209 F1 (NETZSCH Instruments Co., Ltd., Germany) thermogravimetric analyzer with a heating rate of 20 °C/min in an air atmosphere. FTIR spectra were recorded using a Nicolet 5700 spectrometer (Thermo Nicolet Corp.) at a wavenumber range of 4000-650 cm^{-1} under ambient conditions. The mechanical properties of the electrospun mats were examined using a materials testing machine (H5K–S, Hounsfield, UK) with an elongation speed of 10 mm/min at 20 °C and a relative humidity of 63%. Before measurements, 5 pieces of rectangular nanofibrous mats were cut into a dimension of 10 mm× 50 mm according to literature.[36] The apparent density and porosity of electrospun mats before and after treatment were calculated using eq 1 and 2,[26] respectively, where the thickness of the nanofibrous mats was measured by a micrometer and the bulk density of the mats was calculated according to the polymer weight ratio in the mixture.

$$\text{apparent density (g/cm}^3\text{)} = \frac{\text{mat mass (g)}}{\text{mat thickness (cm)} \times \text{mat area (cm}^2\text{)}} \quad (1)$$

$$\text{porosity} = \left\{1 - \frac{\text{mat apparent density (g/cm}^3\text{)}}{\text{bulk density of mixture (g/cm}^3\text{)}}\right\} \times 100\% \quad (2)$$

Catalysis Experiments. The catalytic reduction of Cr(VI) to Cr(III) was performed to evaluate the catalytic efficiency and reusability of Pd NP-immobilized PEI/PVA nanofibrous mats according to a procedure reported in the literature[13] but with some modifications. A mixture solution containing water (24 mL), $K_2Cr_2O_7$ solution (3 mM, 15 mL), and formic acid (88%, 1.5 mL) was first prepared in a 100-mL glass beaker at a water bath with a temperature of 50 °C, and then a piece of Pd NP-containing PEI/PVA nanofibrous mat (2.3 mg, 1×1 cm^2) was immersed into the mixture solution, followed by gentle magnetic stirring. At each predetermined time interval, 1 mL of the aqueous solution was withdrawn and diluted to 2 mL for the analysis of transformation efficiency of Cr(VI) to Cr(III) using a Lambda 25 UV-Vis spectrometer (Perkin Elmer, United States). After one complete reaction cycle, the Pd NP-containing PEI/PVA nanofibrous mat was washed with DI water and blotted by a filter paper before it was reused for the next cycle of catalytic reaction. Two control experiments were carried out under similar conditions for comparison: (1) the cross-linked freestanding PEI/PVA nanofibrous mats without Pd NPs were used in the same reaction, and (2) the same reaction was carried out in the absence of nanofibrous mats or catalyst.

RESULTS AND DISCUSSION

Formation of Water-Stable Electrospun PEI/PVA Nanofibers. It is well known that the uniformity of electrospun nanofibers is greatly influenced by the polymer solution properties and the electrospinning processing parameters. In our previous study,[9] we optimized the electrospinning conditions to fabricate uniform PEI/PVA nanofibrous mats. Under the same optimum experimental parameters (flow rate of 0.3 mL/h, voltage of 18.6 kV, collection distance of 25 cm, and polymer concentration of 12 wt %), smooth and uniform nanofibers with random orientation were generated with a mean diameter of 629 ± 76 nm (Figure 2a). The slightly larger fiber diameter than that reported in our previous study (490 ± 83 nm)[9] may be due to the use of different electrospinning equipments. For immobilization of Pd NPs within the nanofibrous mats, the PEI/PVA nanofibers have to be cross-linked to render them with good water stability. Since the aldehyde groups of GA is proven to be able to interact with the amine groups of PEI and the hydroxyl groups of PVA, GA vapor was used to cross-link the prepared nanofibers to gain water stability, similar to our previous study.[9]

The morphology of the cross-linked PEI/PVA nanofibers was observed via SEM (Figure 2b). It is clear that when compared with the pristine nanofibers before cross-linking (Figure 2a), smooth and uniform fibrous structures are well-retained, except for an obvious increase in the mean fiber diameter (785 ± 81 nm). This can be ascribed to the swelling of the fibers during the GA vapor cross-linking process,[35] in agreement with our previous study.[9] The cross-linked PEI/PVA nanofibers exhibited excellent stability even after immersion in water for a month.

Pd NP-Containing PEI/PVA Nanofibers. After immersion of the PEI/PVA nanofibrous mats in the K_2PdCl_4 solution, the $PdCl_4^{2-}$ anions are able to bind with the available amine groups of PEI via electrostatic interaction, similar to the case of binding of $AuCl_4^-$ ions as reported in our previous study.[9] Upon an addition of the reducing agent $NaBH_4$, Pd NPs were formed and immobilized within the electrospun nanofibrous mats. A photograph of the PEI/PVA nanofibrous mat before and after Pd NP immobilization reveals the color change of the mat from light yellow to dark brown (see Figure S1 in the Supporting Information), confirming the formation of Pd NPs within the nanofibers. SEM, TEM, FTIR, EDS, and TGA were used to fully characterize the Pd NP-containing PEI/PVA nanofibrous mats.

Figure 2c shows a typical SEM image and the diameter distribution histogram of the Pd NP-containing nanofibrous mats. It is clear that the composite nanofibrous mats still retain uniform fibrous structure with a smooth surface, similar to the nanofibers without Pd NPs (Figure 2a, b). Compared to the cross-linked PEI/PVA nanofibers without Pd NPs (785 ± 81 nm), the diameter of Pd NP-containing nanofibers (791 ± 90 nm) is slightly larger, which is likely due to the incorporation of Pd NPs and the slight fiber swelling during the NP loading and fiber washing process, in agreement with our previous work.[9]

Figure 3 shows the cross-sectional TEM images of Pd NP-containing PEI/PVA nanofibers and the size distribution

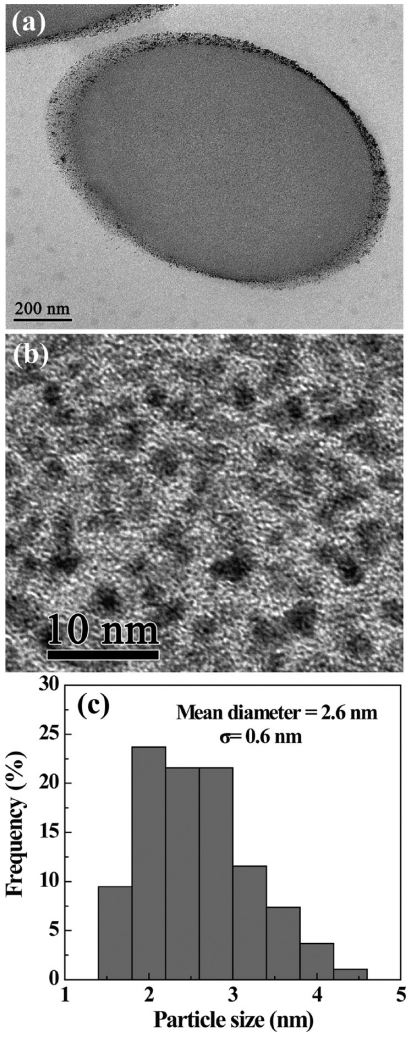

Figure 3. (a) Cross-sectional TEM image and (b) high-resolution TEM image of Pd NP-containing PEI/PVA nanofibers. (c) Size distribution histogram of the immobilized Pd NPs.

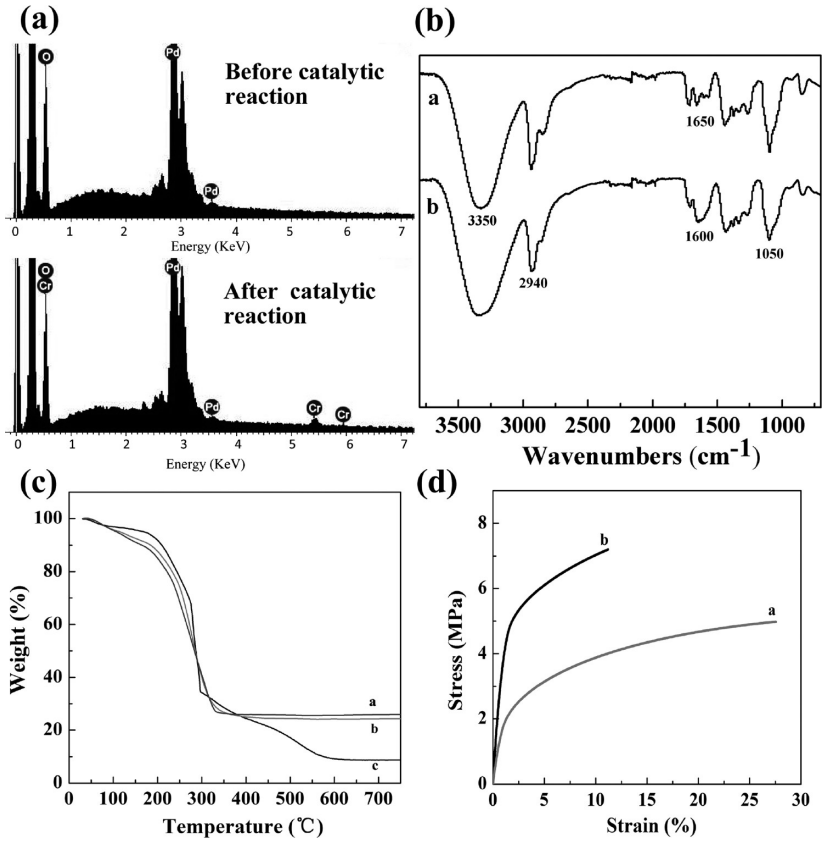

Figure 4. (a) EDS spectra of the Pd NP-containing PEI/PVA nanofibers before and after 3 catalysis reaction cycles. (b) FTIR spectra of the GA vapor-cross-linked nanofibers (Curve a) and Pd NP-immobilized nanofibers (curve b). (c) TGA curves of the Pd NP-immobilized cross-linked PEI/PVA nanofibers (curve a) and the same nanofibers after 3 catalytic reaction cycles (Curve b). Curve c represents the cross-linked PEI/PVA nanofibrous mats before Pd NP immobilization. (d) Stress−strain curves of the GA vapor cross-linked PEI/PVA nanofibrous mats (curve a) and Pd NP-immobilized PEI/PVA nanofibrous mats (curve b).

histogram of the Pd NPs formed in the nanofibers. Round-shaped patterns of Pd NPs with a relatively uniform distribution are clearly observed, indicating that Pd NPs are successfully formed along the cross section of the fibers (Figure 3a). The size distribution histogram of the Pd NPs (Figure 3c) on the basis of the measurement of 300 randomly selected Pd NPs suggests that the formed Pd NPs have a narrow size distribution ranging from 1 to 5 nm and the mean diameter of the Pd NPs was estimated to be 2.6 nm. Different from our previous study related to the uniform distribution of AuNPs within the PEI/PVA nanofibers,[9] we notice that the Pd NPs have a denser distribution at the outer shell of the fibers than in the central area of the fibers. This could be due to the higher concentration of $PdCl_4^{2-}$ used to complex with the PEI amines in the nanofibers than that of $AuCl_4^-$ for immobilization of AuNPs reported in our previous study.[9] Therefore, the outer shell of the nanofibers has more chances to complex more $PdCl_4^{2-}$ ions, leading to a much denser distribution of the Pd NPs in the outer shell of the nanofibers. A high-resolution TEM image of the fiber section clearly shows that individual Pd NPs are uniformly distributed in the interior part of the nanofibers (Figure 3b). It should be noted that the size of the immobilized Pd NPs may be tuned by varying the initial K_2PdCl_4 concentration or by varying the addition rate of $NaBH_4$ solution.

The elemental composition of the Pd NP-immobilized PEI/PVA nanofibrous mats was confirmed by EDS (Figure 4a). The existence of the Pd element demonstrates the successful immobilization of Pd NPs within the nanofibers. The elemental oxygen can be attributed to the hydroxyl groups of the PVA polymer in the nanofibers, and the chlorine signal is from the generated NaCl residue during the Pd NP immobilization process.

FTIR spectroscopy was used to characterize the cross-linked PEI/PVA nanofibers before and after immobilization of Pd NPs (Figure 4b). It is clear that there are still a considerable amount of primary amine groups available (1650 cm^{-1}) in the cross-linked PEI/PVA nanofibers, which is essential for the complexation of $PdCl_4^{2-}$ anions. The peaks at 1600 and 1050 cm^{-1} are indicative of the aldimine and ether linkages generated between GA/PEI and GA/PVA after cross-linking, respectively. The methylene groups for both PEI and PVA at 2940 cm^{-1} do not show significant variation after immobilization of Pd NPs. The peaks of O−H and N−H stretching vibrations at 3350 cm^{-1} for the Pd NP-containing nanofibers become broader than that of the cross-linked PEI/PVA nanofibrous mats. This is presumably due to the interaction between the amino/hydroxyl groups of the PEI/PVA polymers and the immobilized Pd NPs.

TGA was used to characterize the loading capacity of Pd NPs in the PEI/PVA nanofibrous mats (Figure 4c). At the temperature above 600 °C, the polymer component of PEI/PVA nanofibrous mats was burned out, and palladium oxide (PdO) residues were left. By comparison of the Pd NP-immobilized nanofibrous mat with those of the Pd-free mat (Figure 4c, curves a and c), the loading capacity of Pd NPs within the nanofibrous mat was estimated to be 13.1%.

Porosity is one of the most important parameters to evaluate the property of electrospun nanofibrous mats with porous structures. Knowing the bulk densities of PEI and PVA polymers, along with the calculated apparent density of the nanofibers, we were able to calculate the porosities of PEI/PVA, cross-linked PEI/PVA, and Pd NP-containing PEI/PVA nanofibrous mats (Table 1). After GA vapor cross-linking, the porosity of PEI/PVA nanofibrous mats increase from 49.3% (for non-cross-linked PEI/PVA nanofibrous mats) to 61.9%, which is presumably due to the swelling of the fibrous structure during the GA vapor cross-linking process. However, after loading with Pd NPs, the porosity of Pd NP-containing polymer nanofibrous mats decreases to 53.0%, which is possibly due to the loading of Pd NPs.

Table 1. Porosities of the Electrospun PEI/PVA Nanofibrous Mats

nanofibrous mats	porosity (%)
PEI/PVA nanofibrous mats	49.3
cross-linked PEI/PVA nanofibrous mats	61.9
Pd NP-containing PEI/PVA nanofibrous mats	53.0

Mechanical durability is of importance for the recovery and reuse of NP-containing fibrous materials in practical catalytic applications. A typical tensile stress-strain curve of the cross-linked PEI/PVA nanofibrous mats before and after loading of Pd NPs is shown in Figure 4d. The mechanical properties in terms of tensile stress, tensile strain, and the Young's modulus are summarized in Table 2. It is clear that the tensile stress of the cross-linked PEI/PVA nanofibers is improved after the loading of Pd NPs. However, the ultimate tensile strain of cross-linked PEI/PVA nanofibrous mats (27.43 ± 6.17%) is decreased after loading of Pd NPs (11.89 ± 3.51%). The Young's modulus of the nanofibrous mats after Pd NP immobilization (290.68 ± 16.97 MPa) is largely improved when compared with that of the cross-linked nanofibrous mats without Pd NPs (189.34 ± 6.94 MPa). This could be due to the efficient load transfer from the polymer fibers to the immobilized Pd NPs, in agreement with our previous results related to other NP-incorporated nanofibers.[33,37,38]

Table 2. Mechanical Properties of the PEI/PVA Nanofibrous Mats

nanofibrous mats	tensile stress (MPa)	tensile strain (%)	Young's modulus (MPa)
cross-linked nanofibrous mats	4.88 ± 0.74	27.43 ± 6.17	189.34 ± 6.94
Pd NP-containing nanofibrous mats	7.19 ± 1.44	11.89 ± 3.51	290.68 ± 16.97

Catalytic Activity of Pd NP-Immobilized PEI/PVA Nanofibers. The catalytic activity of the Pd NP-immobilized PEI/PVA nanofibrous mats was investigated by transformation of toxic Cr(VI) to Cr(III) in the presence of formic acid as a reducing agent at 50 °C. $K_2Cr_2O_7$ was chosen as one of the representative Cr(VI) sources and the Cr(VI) reduction process was monitored by UV−vis spectroscopy. It is believed that the adsorption of both chromate and hydrogen donor (formic acid) on the surface of the Pd NPs leads to the redox degradation of formic acid into carbon dioxide and hydrogen, consequently reducing Cr(VI) to Cr(III) through hydrogen transfer. With the immobilization of Pd NPs within PEI/PVA nanofibers, it is expected that Pd NPs could work more effectively due to the higher surface-area-to-volume ratio of the nanofibers, the permeability of the nanofibers allowing for efficient access of the small molecules, and less aggregation of Pd NPs within nanofiber matrix. The catalytic performance of the Pd NP-immobilized PEI/PVA nanofibrous mats was first confirmed by visual observation of the color fading from yellow to colorless within 12 min, indicating the efficient transformation of Cr(VI) (yellow color) to Cr(III) (colorless) (see Figure S2 in the Supporting Information). The intensity of the characteristic absorption peak at 350 nm for $Cr_2O_7^{2-}$ which is due to the ligand (oxygen) to metal (Cr(VI)) charge transfer[39] decreases with time, confirming the quick reduction of Cr(VI) (Figure 5a). At 50 °C, it took about 12 min for the absorption peak at 350 nm to vanish, which indicates the completeness of the reduction reaction. The ultimate transformation efficiency was estimated to be 99.7% within 12 min. The presence of Cr(III) as the reaction product was confirmed by adding an excess of sodium hydroxide solution, where an emergence of a green color indicates the formation of hexahydroxochromate (III). Notably, the catalytic activity of the Pd NP-immobilized PEI/PVA nanofibrous is solely related to the immobilized Pd NPs. A control experiment to transform Cr(VI) to Cr(III) using PEI/PVA nanofibrous mats without Pd NPs in the presence of formic acid did not give rise to an efficient spectral change of the Cr(VI) absorption (Figure 5b). The slight peak intensity decrease after 25 min may be related to the adsorption of $Cr_2O_7^{2-}$ ions onto the PEI/PVA nanofibers driven by electrostatic interaction between negatively charged $Cr_2O_7^{2-}$ ions and the positively charged PEI amines. Additionally, the

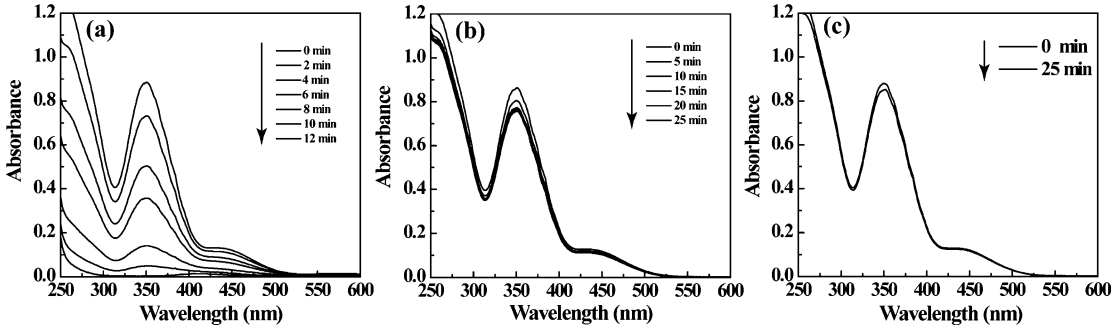

Figure 5. UV−vis spectra of Cr(VI) aqueous solution (a) treated with the Pd NP-immobilized PEI/PVA nanofibrous mat in the presence of formic acid, (b) treated with the PEI/PVA nanofibrous mat without Pd NPs in the presence of formic acid, and (c) treated with only formic acid, respectively.

Cr(VI) aqueous solution treated by formic acid only did not have any significant decrease in the absorption intensity at 350 nm within 25 min, suggesting that the reaction to transform Cr(VI) to Cr(III) does not occur without catalysts (Figure 5c). These results further confirmed that the superior catalytic transformation of Cr(VI) is solely attributed to the immobilized Pd NPs within the PEI/PVA nanofibers. Compared with the Pd NP-supported mesoporous Al_2O_3 films with a transformation efficiency of >98% within 40 min,[13] our Pd NP-immobilized polymer nanofibers are much more efficient with a transformation efficiency of 99.7% within 12 min.

The reusability and recyclability are crucial issues for a catalyst to be used for practical applications, especially for the costly rare and noble metals (e.g., Pd and Au). The formed freestanding Pd NP-immobilized PEI/PVA nanofibrous mats with good mechanical durability are essential for them to be recycled for multiple catalytic uses. After each reaction cycle, the mat was washed with water and blotted by a filter paper before it was reused for the next cycle of catalytic reaction. The catalytic performance of the Pd NP-immobilized PEI/PVA nanofibrous mats used for 3 different times was compared by plotting the remaining fraction of Cr(VI) as a function of reaction time (Figure 6). It can be seen that more than 99%

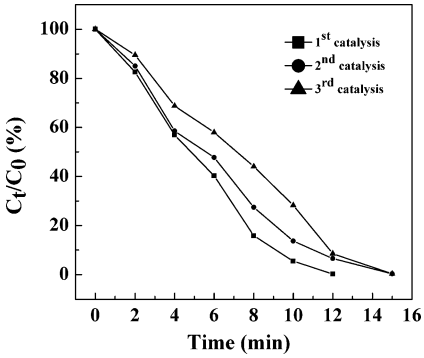

Figure 6. Remaining fraction of Cr(VI) as a function of reaction time in the presence of the Pd NP-immobilized PEI/PVA nanofibrous mat as the catalyst for the first, second, and third catalytic reaction cycles.

Cr(VI) is able to be transformed to Cr(III) after 12, 15, and 15 min for the 1st, 2nd, and 3rd reaction cycles, respectively, confirming the excellent reusability of the Pd NP-containing PEI/PVA fibrous mat. The very slight deterioration of the catalytic performance after each previous reaction cycle could be due to the formation of PdH_x species. The hydrogen formed by the decomposition of HCOOH could be adsorbed on the surface of the Pd NPs, resulting in the formation of palladium hydride (PdH_x).[40] It should be noted that the catalytic activity of Pd NPs immobilized within the nanofibers may be fully restored by heating the Pd NPs at 180 °C to remove the hydrogen species according to the work reported by Phan and coworkers.[40] However, due to the fact that the polymer nanofibers start to decompose at the temperature of 180 °C (Figure 4c), it remains difficult to fully restore the catalytic activity of Pd NPs by such heating treatment.

The stability of the Pd NP-containing PEI/PVA nanofibers is very important for their uses as a highly efficient catalyst. After 3 catalytic reaction cycles, the morphology and the composition of the Pd NP-immobilized nanofibers were checked and characterized by SEM, EDS, and TGA, respectively. We show that the porous nanofibrous structure of the Pd NP-immobilized PEI/PVA nanofibrous mats is well retained, similar to that of the same mats before catalytic uses (Figure 7). In addition, after 3 cycles of catalytic reaction, the Pd NP-

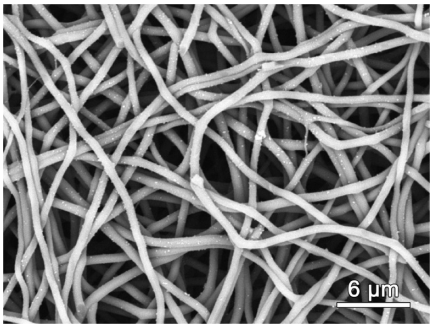

Figure 7. SEM micrograph of the Pd NP-immobilized PEI/PVA nanofibers after 3 catalytic reaction cycles.

containing PEI/PVA nanofibers display the similar Pd signals shown in the EDS spectrum with Cr residues (Figure 4a) and the similar weight loss in the TGA curve (Figure 4c, Curve b), respectively to those of the fibers before use as a catalyst. All of these characterization data indicate that the Pd NP-immobilized PEI/PVA nanofibers are very stable and do not release the Pd species from the nanofiber matrix even after undergoing multiple catalytic reaction cycles.

CONCLUSION

In summary, we have developed a facile approach to simultaneously synthesizing and immobilizing Pd NPs within PEI/PVA nanofibrous mats. The immobilization of the Pd NPs with a mean diameter of 2.6 nm within the PEI/PVA nanofibers does not impact the porous fibrous structure of the mats. The formed composite Pd NP-containing nanofibrous mats with a mean diameter of 791 nm are stable in water and have a porosity of 53.0%. The catalytic reaction to transform Cr(VI) to Cr(III) demonstrates that the Pd NPs immobilized within the nanofibrous mats are able to catalyze the Cr(VI) reducing reaction with an efficiency approaching 99.7% within 12 min at 50 °C. Furthermore, the Pd NP-containing PEI/PVA nanofibrous mats can be easily handled and reused for at least 3 times with approximately similar catalytic performance. These findings provide new thoughts or avenues for fabricating highly efficient nanofiber-based cost-effective catalysts for various catalytic applications.

ASSOCIATED CONTENT

Supporting Information

Additional photograph of the PEI/PVA nanofibrous mats before and after Pd NP immobilization and photograph of the Cr(VI) aqueous solution reduced by formic acid in the presence of the catalyst of Pd NP-immobilized PEI/PVA nanofibrous mat at different time intervals. This material is available free of charge via the Internet at http://pubs.acs.org.

AUTHOR INFORMATION

Corresponding Author

*E-mail: mwshen@dhu.edu.cn (M.S.); xshi@dhu.edu.cn (X.S.).

Notes

The authors declare no competing financial interest.

■ ACKNOWLEDGMENTS

This research is financially supported by Fundamental Research Funds for the Central Universities (for M.S, R.G., X.C., and X.S.), the Program for New Century Excellent Talents in University, State Education Ministry, the Program for Professor of Special Appointment (Eastern Scholar) at Shanghai Institutions of Higher Learning, and the Key Laboratory of Textile Science & Technology, Ministry of Education, "111 Project", B07024. X.S. gratefully acknowledges the Fundação para a Ciência e a Tecnologia (FCT) and Santander bank for the Chair in Nanotechnology. M.Z. thanks the National Natural Science Foundation of China (50925312) for support.

■ REFERENCES

(1) Elliott, D. W.; Zhang, W. *Environ. Sci. Technol.* **2001**, *35*, 4922−4926.
(2) Stearns, D. M.; Kennedy, L. J.; Courtney, K. D.; Giangrande, P. H.; Phieffer, L. S.; Wetterhahn, K. E. *Biochemistry* **1995**, *34*, 910−919.
(3) Omole, M. A.; Okello, V. A.; Lee, V.; Zhou, L.; Sadik, O. A. *ACS Catal.* **2011**, *1*, 139−146.
(4) Park, D.; Yun, Y.-S.; Park, J. M. *Environ. Sci. Technol.* **2004**, *38*, 4860−4864.
(5) Patterson, R. R.; Fendorf, S. *Environ. Sci. Technol.* **1997**, *31*, 2039−2044.
(6) Daneshvar, N.; Salari, D.; Aber, S. *J. Hazard. Mater.* **2002**, *94*, 49−61.
(7) Puzon, G. J.; Roberts, A. G.; Kramer, D. M.; Xun, L. *Environ. Sci. Technol.* **2005**, *39*, 2811−2817.
(8) Du, J.; Qi, J.; Wang, D.; Tang, Z. *Energy Environ. Sci.* **2012**, *5*, 6914−6918.
(9) Fang, X.; Ma, H.; Xiao, S.; Shen, M.; Guo, R.; Cao, X.; Shi, X. *J. Mater. Chem.* **2011**, *21*, 4493−4501.
(10) Ma, H.; Huang, Y.; Shen, M.; Guo, R.; Cao, X.; Shi, X. *J. Hazard. Mater.* **2012**, *211-212*, 349−356.
(11) Wang, J.; Gong, J.; Xiong, Y.; Yang, J.; Gao, Y.; Liu, Y.; Lu, X.; Tang, Z. *Chem. Commun.* **2011**, *47*, 6894−6896.
(12) Omole, M. A.; K'Owino, I. O.; Sadik, O. A. *Appl. Catal. B* **2007**, *76*, 158−167.
(13) Dandapat, A.; Jana, D.; De, G. *Appl. Catal. A* **2011**, *396*, 34−39.
(14) Hou, H.; Reneker, D. H. *Adv. Mater.* **2004**, *16*, 69−73.
(15) Li, D.; Xia, Y. *Adv. Mater.* **2004**, *16*, 1151−1170.
(16) Kim, B.; Park, H.; Lee, S.-H.; Sigmund, W. M. *Mater. Lett.* **2005**, *59*, 829−832.
(17) Reneker, D. H.; Yarin, A. L. *Polymer* **2008**, *49*, 2387−2425.
(18) Yoon, K.; Hsiao, B. S.; Chu, B. *J. Mater. Chem.* **2008**, *18*, 5326−5334.
(19) Fujihara, K.; Kumar, A.; Jose, R.; Ramakrishna, S.; Uchida, S. *Nanotechnology* **2007**, *18*, 365709.
(20) Lebrun, L.; Vallée, F.; Alexandre, B.; Nguyen, Q. T. *Desalination* **2007**, *207*, 9−23.
(21) Fang, X.; Xiao, S.; Shen, M.; Guo, R.; Wang, S.; Shi, X. *New J. Chem.* **2011**, *35*, 360−368.
(22) Xiao, S.; Ma, H.; Shen, M.; Wang, S.; Huang, Q.; Shi, X. *Colloid Surf. A* **2011**, *381*, 48−54.
(23) Xiao, S.; Shen, M.; Ma, H.; Fang, X.; Huang, Q.; Weber, W. J., Jr.; Shi, X. *J. Nanosci. Nanotechnol.* **2011**, *11*, 5089−5097.
(24) Schreuder-Gibson, H.; Gibson, P.; Senecal, K.; Sennett, M.; Walker, J.; Yeomans, W.; Ziegler, D.; Tsai, P. P. *J. Adv. Mater.* **2001**, *34*, 44−55.
(25) Wang, X.; Kim, Y.-G.; Drew, C.; Ku, B.-C.; Kumar, J.; Samuelson, L. A. *Nano Lett.* **2004**, *4*, 331−334.
(26) He, W.; Ma, Z. W.; Yong, T.; Teo, W. E.; Ramakrishna, S. *Biomaterials* **2005**, *26*, 7606−7615.
(27) Hong, K. H. *Polym. Eng. Sci.* **2007**, *47*, 43−49.
(28) Liao, H.; Qi, R.; Shen, M.; Cao, X.; Guo, R.; Zhang, Y.; Shi, X. *Colloid Surf. B* **2011**, *84*, 528−535.
(29) Liu, F.; Guo, R.; Shen, M.; Cao, X.; Mo, X.; Wang, S.; Shi, X. *Soft Mater.* **2010**, *8*, 239−253.
(30) Liu, F. J.; Guo, R.; Shen, M. W.; Wang, S. Y.; Shi, X. Y. *Macromol. Mater. Eng.* **2009**, *294*, 666−672.
(31) Wang, S.; Cao, X.; Shen, M.; Guo, R.; Bányai, I.; Shi, X. *Colloid Surf. B* **2012**, *89*, 254−264.
(32) Xiao, S.; Shen, M.; Guo, R.; Wang, S.; Shi, X. *J. Phys. Chem. C* **2009**, *113*, 18062−18068.
(33) Xiao, S.; Shen, M.; Guo, R.; Huang, Q.; Wang, S.; Shi, X. *J. Mater. Chem.* **2010**, *20*, 5700−5708.
(34) Xiao, S.; Wu, S.; Shen, M.; Guo, R.; Huang, Q.; Wang, S.; Shi, X. *ACS Appl. Mater. Interfaces* **2009**, *1*, 2848−2855.
(35) Zhang, Y. Z.; Venugopal, J.; Huang, Z.-M.; Lim, C. T.; Ramakrishna, S. *Polymer* **2006**, *47*, 2911−2917.
(36) Huang, Z. M.; Zhang, Y. Z.; Ramakrishna, S.; Lim, C. T. *Polymer* **2004**, *45*, 5361−5368.
(37) Qi, R.; Cao, X.; Shen, M.; Guo, R.; Yu, J.; Shi, X. *J. Biomater. Sci., Polym. Ed.* **2012**, *23*, 299−313.
(38) Qi, R.; Guo, R.; Shen, M.; Cao, X.; Zhang, L.; Xu, J.; Yu, J.; Shi, X. *J. Mater. Chem.* **2010**, *20*, 10622−10629.
(39) Chlistunoff, J. B.; Johnston, K. P. *J. Phys. Chem. B* **1998**, *102*, 3993−4003.
(40) Phan, T.-H.; Schaak, R. E. *Chem. Commun.* **2009**, 3026−3028.